Chinese Journal of Polymer Science Vol. 35, No. 6, (2017), 782−792

Chinese Journal of Polymer Science
© Chinese Chemical Society
Institute of Chemistry, CAS
Springer-Verlag Berlin Heidelberg 2017

Isothermal-crystallization Kinetics and Spherulite Growth of Aliphatic Polyketone/Polyamide-6 Blends

He-xin Zhang[a, b], Seong-Rok Huh[a], Eun-Bin Ko[a], Byung-Sik Park[c] and Keun-Byoung Yoon[a*]

[a] *Department of Polymer Science and Engineering, Kyungpook National University, Korea*
[b] *Key Laboratory of Synthetic Rubber, Changchun Institute of Applied Chemistry, Chinese Academy of Sciences, Changchun 130022, China*
[c] *Department of Pharmaceutical Engineering, International University of Korea, Jinju, Korea*

Abstract In this research, the morphologies, isothermal-crystallization kinetics, and spherulite growth of aliphatic polyketone/polyamide-6 blends were studied. A single glass-transition temperature (T_g) was determined, and the composition dependence of T_g for these blends was well described by the Kwei equation. The strong intermolecular interaction between the two polymer components was confirmed by melting-point depression. The isothermal-crystallization kinetics were analyzed on the basis of the Avrami approach. A linear increase in the radii of the spherulites with time was observed for all compositions. All the spherulites continued to grow at nearly identical growth rates. With increasing polyamide-6 content, the size of the spherulites in the polyketone/polyamide-6 blends gradually decreased, and the number of spherulites in the blends increased.

Keywords Polyketone; Polyamide-6; Crystallization kinetics; Spherulite growth

Electronic Supplementary Material Supplementary material is available in the online version of this article at http://dx.doi.org/10.1007/s10118-017-1936-3.

INTRODUCTION

Polymers of carbon monoxide and olefins are generally referred to as polyketones (PKs). Of particular interest among PKs is the class of linear alternating polymers of carbon monoxide and at least one ethylenically saturated hydrocarbon[1, 2]. Because of their excellent combination of chemical resistance, mechanical properties, and low gas permeability, certain aliphatic PKs have undergone extensive development as engineering resins in recent years[3]. However, for some applications, properties somewhat different from those of PKs are desirable. It is advantageous to retain the more desirable properties of PKs and improve other properties. These advantages are often provision of polymer blends.

Polymer blends have been widely used for engineering purposes. The excellent physical/mechanical properties of polymer blends, such as high impact resistance, high modulus, or strong toughness, are closely related to the highly controlled or ordered morphology and homogeneity of the raw materials used. Asano *et al.*[4] reported that semicrystalline PK/polyamide-6 (PK/PA-6) blends obtained by a simple blending process exhibit better impact properties than those expected from the simple addition of the impact energies of both PK and PA-6 under wet conditions. Asano *et al.*[5] and Kato *et al.*[6] recently reported that aliphatic PK and PA-6 blends have an enhanced Charpy impact energy greater than that of polycarbonate, as a result of moisture

* Corresponding author: Keun-Byoung Yoon, E-mail: kbyoon@knu.ac.kr
Received December 17, 2016; Revised December 28, 2016; Accepted January 23, 2017
doi: 10.1007/s10118-017-1936-3

absorption. They observed PK-rich and PA-rich phases at the nanometer level in the blends as well as the formation of a co-continuous nano-layer from the PA-rich phase and the lamellar network of the PK-rich phase. Aliphatic PK and PA-6 is a well-known miscible blend system. Although extensive research has focused on aliphatic PK blends, there is little attention paid to the isothermal and non-isothermal crystallization kinetics of aliphatic PK/PA-6 blend system.

In this study, we blended aliphatic PK with various amounts of PA-6 and studied the crystallization kinetics and spherulite growth of blends with different compositions. The interaction parameters of PK and PA-6 were evaluated using the equilibrium melting-point depression. This is the first report to discuss in detail the parameters of the isothermal-crystallization kinetics and the spherulite growth of aliphatic PK/PA-6 blends.

EXPERIMENTAL

Materials and Blends

The aliphatic PK (ethylene/carbon monoxide/propylene terpolymer, C_3: 2.7 mol%) used in this study is commercially available. Its melt index is 60 g/10min. Polyamide-6 (PA-6) is commercial-grade (1027BRT, Hyosung Co., Korea).

Dried PK and PA-6 were blended using a twin-screw mixer (Plasticoder Brabender Company, PLE331). The aliphatic PK and PA-6 were blended at 100 r/min for 5 min at 230 °C. The composition ratios of the aliphatic PK/PA-6 blends maintained were 100/0, 90/10, 80/20, 70/30, 60/40, 50/50, 40/60, 30/70, 20/80, 10/90, and 0/100 (*W*/*W*).

Characterization

The fractured surface and tensile fractured surface morphologies of the PK/PA-6 blends were observed by scanning electron microscopy (SEM, Hitachi, S-4800). The glass-transition temperature (T_g) of the blends was analyzed using a dynamic mechanical analyzer (DMA, PerkinElmer, N535). The dynamic viscoelasticity was analyzed according to the composition ratio of the blends in the temperature range of −40 °C to 100 °C, at a heating rate of 10 K/min and a frequency of 1 Hz.

The crystallization temperature (T_c) and melting temperature (T_m) were measured by using a differential scanning calorimeter (DSC, Setaram, DSC131 evo). The samples were heated to 245 °C and then cooled rapidly to room temperature to remove the thermal history of the semicrystalline polymer. After that T_c and T_m of the samples were measured in a nitrogen atmosphere at a heating rate of 10 K/min in the temperature range of 20 °C to 245 °C.

The melt flow index (MI) was measured by Melt Indexer (MP-MPX62.92, Göttfert, Germany) at 230 °C for 2 min at a constant load (2.16 kg) (ASTM D1238).

The spherulitic morphologies and growth rates of the PK and PK/PA-6 blends were observed on films (thickness about 100 μm) using a polarized optical microscope equipped with an automatic thermal control hot-stage (POM, Nikon Eclipse, E400).

Tensile test was performed on a screw-driven universal testing machine (Instron 4466) equipped with a 10 kN electronic load cell and mechanical grips. All tests were carried out according to the ASTM standards, and five replicates were tested for each sample to get an average value. Specimens were prepared by using a hot press at 230 °C, a hold pressure of 7 MPa and a hold time of 2 min. The sample size for the tensile drawing experiment was 5.0 mm × 75.0 mm × 1.0 mm. The sample gauge length was 25.0 mm, and the crosshead speed was 10.0 mm/min.

Infrared spectra of the blends were recorded on a Fourier transform infrared spectrometer (FTIR, Jasco FTIR-4100). The spectra were recorded at room temperature with 4 cm^{-1} resolution and averaged over 16 scans in the 4000–400 cm^{-1} range.

RESULTS AND DISCUSSION

Morphologies and Glass-transition Temperature of Blends

The fractured-surface morphologies of the PK/PA-6 blends were observed by SEM. Figure 1 shows SEM photomicrographs of the fractured surface of the PK/PA-6 blends. No phase-separated phenomena occurred; the blends had a micro-level homogeneous phase for all compositions, and the entire contents appeared in just one phase, indicating strong interfacial adhesion between the PK and PA-6.

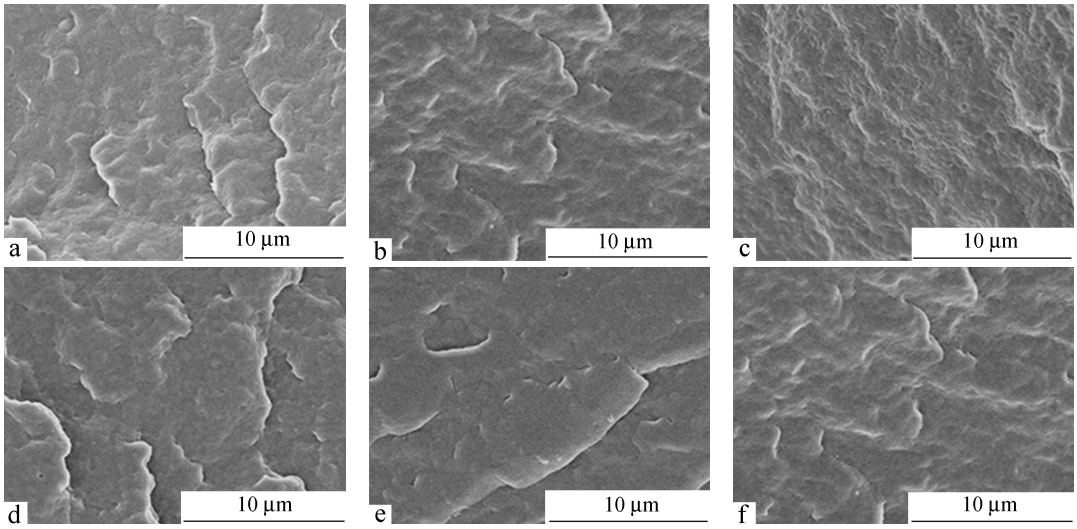


Fig. 1 SEM images of the fractured surfaces of PK/PA-6 blends: (a) 100/0, (b) 90/10, (c) 70/30, (d) 50/50, (e) 30/70 and (f) 10/90

To further explore the miscibility of PK and PA-6, the tensile-fractured surfaces along the tensile direction were observed by SEM, and the results are shown in Fig. 2. The tensile-fractured surface of PK exhibited highly elongated PK fibrils and a large degree of deformation, indicating that a brittle-to-ductile transition occurred. With the addition of PA-6, the degree of the PK matrix deformation gradually reduced. For the PA-6 enriched samples (Figs. 2e and 2f), the tensile-fractured surfaces tended to be roughly flat and smooth. During the tensile

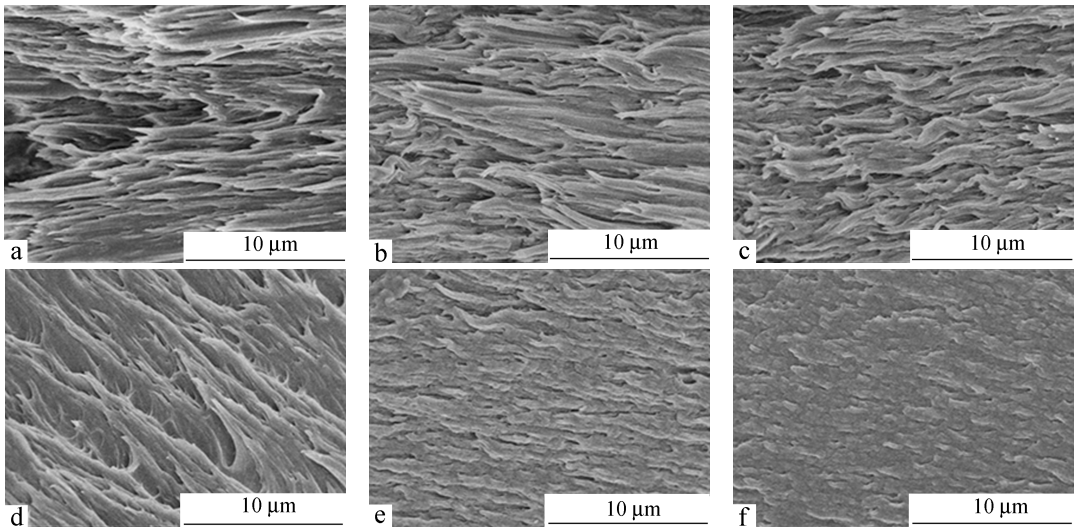


Fig. 2 SEM images of the tensile fractured surfaces of PK/PA-6 blends: (a) 100/0, (b) 90/10, (c) 70/30, (d) 50/50, (e) 30/70, and (f) 10/90

process, PA-6, which had a far lower elastic modulus than PK, could not deform easily and reduced the matrix shear yielding under the support of excellent interfacial interaction. Although the weight ratio of PA-6 was changed from 10 wt% to 90 wt%, good interfacial adhesion was maintained between the PK and PA-6 phases. It was confirmed that the aliphatic PK and PA-6 blends were well-mixed and exhibited homogeneous morphologies. Meanwhile, the modulus of PK slightly increased but tensile strength did not change basically with increasing amount of PA-6 added, as shown in Fig. 3.

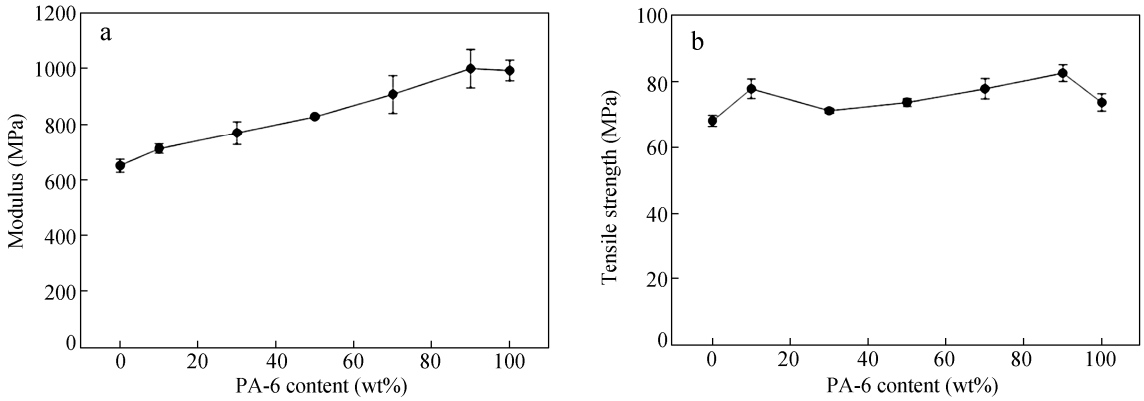


Fig. 3 Effect of PA-6 content on modulus (a) and tensile strength (b) of PK/PA-6

Dynamic mechanical analysis is typically used to study the phase behavior of binary blends, as this technique is very sensitive to molecular relaxation process. Changing the degree of mutual solubility of the component polymers affected the transitions, providing direct evidence of the miscibility. As shown in Fig. 4, the neat PK and PA-6 show distinguishable T_g values of approximately −7.2 and 49.0 °C, respectively. The T_g values of the blends are located between those of PK and PA-6. Thus, the two components were miscible over the entire composition range.

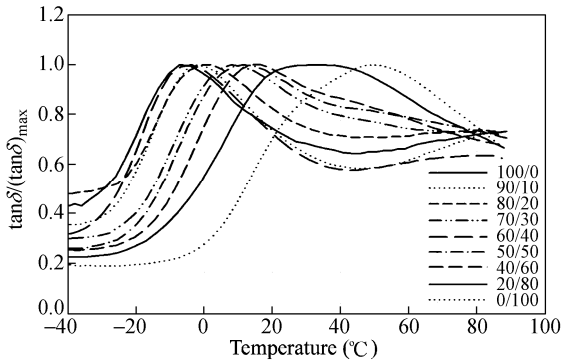


Fig. 4 tanδ of PK/PA-6 blends (analysis using DMA)

A number of equations have been proposed for relating the T_g of a miscible blend to the composition and T_g of its constituents. The results are presented in Fig. 5 and Table S1 (in supporting information, SI). The apparent asymmetry in the curve indicates that the widely used classical Fox equation[7] and a similar treatment can also be applied by using a common alternative to the Gordon-Taylor equation[8, 9]. Although these equations have been successfully applied to certain blends, some systems still exhibit significant deviations; systems containing hydrogen bonding exhibit particularly severe deviations. With regard to PK/PA-6 blends, the most suitable relationship is the Kwei equation[10, 11]. The composition dependence of T_g for the PK/PA-6 blend system agrees well with the Kwei equation. The PK and PA-6 components are considered to interact in the blends for all compositions. This favorable interaction is the direct reason for the pseudo-negative deviation of T_g versus the

composition, according to the simple mixing rule[12].

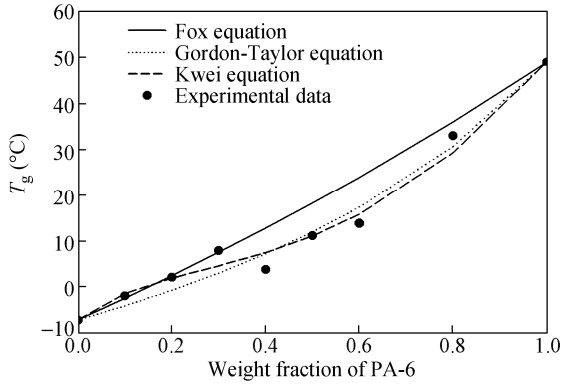


Fig. 5 Composition dependence of T_g for the PK/PA-6 blend

Interaction between PK and PA-6

The interaction between PK and PA-6 in the blends was further investigated using the well-known melting-point depression method. The depression in the melting point of the crystalline component in polymer blends can reveal important information about the miscibility and polymer-polymer interaction parameters. The equilibrium melting temperature for the blends was obtained using the classical Hoffman-Weeks method[13]. This method obtains the equilibrium melting temperature (T^0_m) of a polymer *via* extending a plot of measured T_m versus the temperature at which the sample is crystallized (T_c) to the line corresponding to $T_m = T_c$.

Figure 6 presents Hoffman-Weeks plots for PK and its blends with PA-6. A linear dependence of T_m on T_c is observed for all compositions. The equilibrium melting point decreased as the amount of PA-6 in the blend increased. The melting-point depression of the crystalline-polymer component in a binary blend depends on the strength of the thermodynamic interaction between the two components[12]. For immiscible or partially miscible polymer blends, the equilibrium melting point of the crystalline-polymer component is generally not depressed. Depression of the equilibrium melting point is typically observed in miscible blends because of the favorable interaction between the components. Therefore, the T^0_m values of pure PK and PK/PA-6 (50/50) are determined to be 231.3 and 226.7 °C, respectively. The depression of T^0_m provides additional evidence for miscibility between aliphtic PK and PA-6.

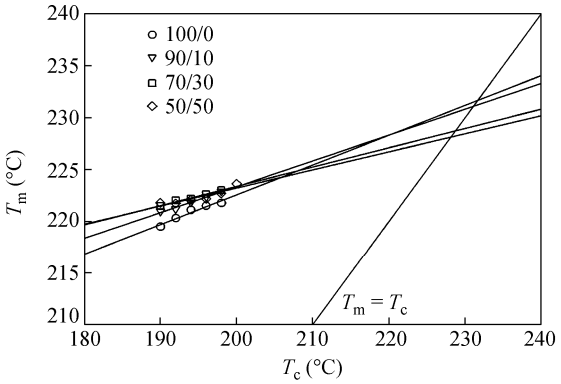


Fig. 6 Hoffman-Weeks plot of PK/PA-6 blends

Determination of the melting-point depression of the crystalline component in a binary blend can contribute to the assessment of the Flory-Huggins interaction parameter (χ_{12}) between the blending components[14, 15]. The χ_{12} value between PK and PA-6 was calculated using the Flory-Huggins relationship as follows:

$$(1/T^0_{mB} - 1/T^0_{mP}) = -RV_2/\Delta H^0_f V_1[\ln\varphi_1/m_2 + (1/m_2 - 1/m_1)\varphi_1 + \chi_{12}\varphi_1^2] \quad (1)$$

where T^0_{mP} and T^0_{mB} are the equilibrium melting temperatures of the crystallizable component of polymer and the blend, respectively; V_1 (= 104.24 cm^3/mol) and V_2 (= 45.16 cm^3/mol) are the molar volumes of PA-6 and PK, respectively; H^0_f (= 13053 J/mol) is the heat of fusion per mole of the perfectly crystallizable PK per repeat unit; and φ_1 is the volume fraction of PA-6[16, 17].

When the molecular weight of the polymer is high, $\ln\varphi_1/m_2$, $1/m_1$, and $1/m_2$ can be ignored. Therefore, the related terms in Eq. (1) can be neglected, and the interaction parameter χ_{12} is written as follows[18–20]:

$$-[\Delta H^0_f V_1/RV_2(1/T^0_{mB} - 1/T^0_{mP})] = \chi_{12}\varphi_1^2 \quad (2)$$

The equilibrium melting temperature of the crystallizable component can indicate the interaction parameter of the blends. The resulting value is $\chi_{12} = -0.72$, which means that the aliphatic PK and PA-6 blend system is thermodynamically miscible.

The interaction between PK and PA-6 was also investigated by Fourier transform infrared (FTIR) spectroscopy. Figure 7 shows the FTIR spectra of the PK, PA-6, and PK/PA-6 blends. As the PA-6 content increased, the peak intensity of NHC=O stretching (1633 cm^{-1}) and N−H bending (1538 cm^{-1}) of PA-6 increased, and the intensity of C=O stretching (1699 cm^{-1}) in PK decreased. Additionally, as the PA-6 content increased, the C=O peak of PK shifted toward a high frequency, whereas the NHC=O and N−H peaks shifted toward a low frequency. To explain the significant change in the FTIR peak position, we suggest that reactions occurred between the PK and PA-6 blends.

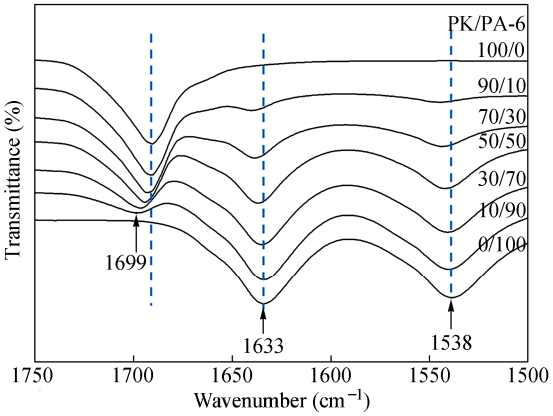


Fig. 7 FTIR spectra of the PK/PA-6 blends

Isothermal-crystallization Kinetics

The polymer crystallization process is a function of both thermodynamic and kinetic factors, but the latter ones usually dominate. The physical, chemical and mechanical properties of crystalline polymers depend on the morphology, crystalline structure and degree of crystallization. In order to control the rate of the crystallization and to obtain the desired morphology and properties, a great deal of efforts has been devoted to studying the crystallization kinetics and determining the change in properties[21–23]. Therefore, it is important to investigate both the quiescent and dynamic crystallization kinetics of the crystalline polymers. Crystallization kinetics is very important for the selection of processing parameters such as the mold temperature and hold time in injection molding[24–26]. Isothermal crystallization was performed by rapidly cooling the sample from the melt temperature to the crystallization temperature, and then the heat evolved was measured while the sample was held under isothermal conditions. Typical isothermal crystallization exotherms and relative crystallinity of the PK/PA-6 (70/30) blend are shown in Fig. 8 (Figs. S1 and S2 in SI).

Obviously, the crystallization process was strongly influenced by T_c, *i.e.*, the crystallization rate decreased as T_c increased. The crystallization exothermic peak became flatter, and the time taken to reach the maximum degree of crystallization increased with the crystallization temperature. The crystallization exothermic peak of PK became sharp with the addition of PA-6 at the same T_c.

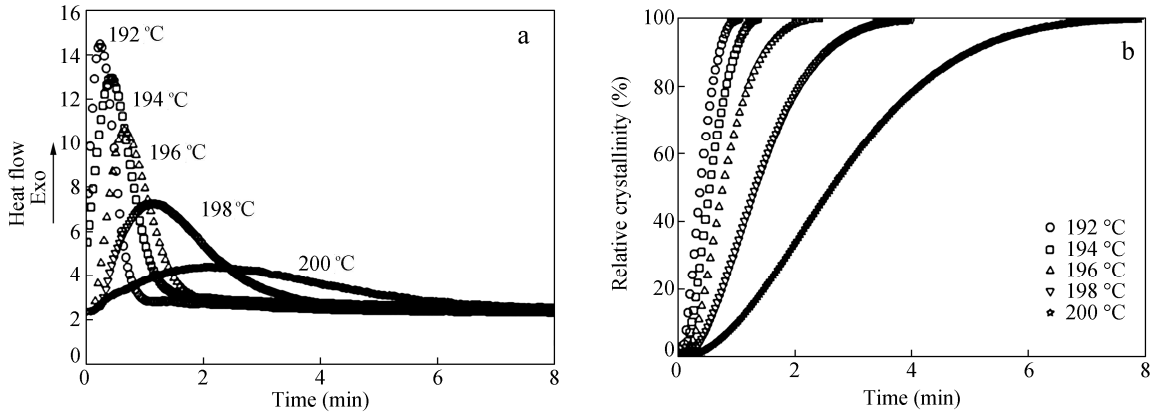


Fig. 8 Isothermal-crystallization curves (a) and relative crystallinity-versus-time curves (b) of a selected PK/PA-6 (70/30) blend at various crystallization temperatures

The isothermal-crystallization kinetics was analyzed by evaluating the degree of crystalline conversion as a function of time at a constant temperature. In Fig. 8(b), the relative crystallinity exhibits a sigmoid dependence. As the crystallization temperature increased, the characteristic isotherms moved to right along the time axis, indicating a lower crystallization rate.

The first nonlinear part of the S-shaped curves is generally considered to represent the induction time and nucleation step in the crystallization process. Each curve shows a linear part that is considered to represent primary crystallization. A second nonlinear part deviates slightly and is considered to represent secondary crystallization, which was caused by spherulite impingement in the later stage of crystal growth.

The Avrami approach is usually employed to analyze the isothermal crystallization kinetics of crystalline polymers[27–29], $1 - X_t = \exp(-kt^n)$, which describes the development of the relative crystallinity X_t in terms of the crystallization time t. The Avrami theory usually provides a good fit of the DSC experimental data at least in the conversion range up to the end of the primary crystallization, that is, up to the impingement of spherulites at approximately 50% conversion to the solid semicrystalline state. The Avrami exponent (n) depends on the nucleation and growth mechanism of the crystals, and the crystal growth-rate constant (k) involves both nucleation and growth-rate parameters[30, 31].

Figures 9 and S3 (in SI) show plots of $\lg[-\ln(1 - X_t)]$ (X_t = 20%–80%) versus $\lg t$ for PK/PA-6 blends crystallized at 190–200 °C. A series of straight lines are observed, indicating that the Avrami method describes the development of the relative degree of crystallinity as a function of the crystallization time very well. The k and n values were obtained directly from the slope and intercept of $\lg[-\ln(1 - X_t)]$ versus $\lg t$, respectively, and the results are summarized in Table 1.

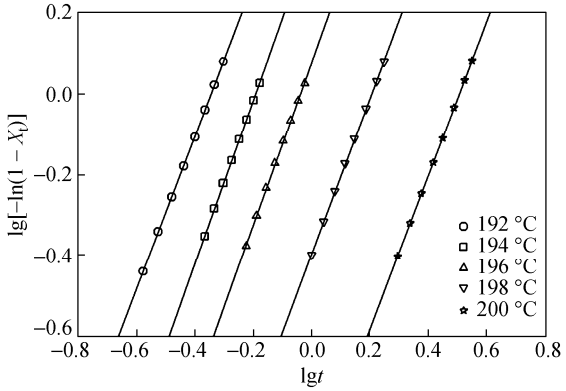


Fig. 9 Avrami plots for the PK/PA-6 (70/30) blend at various temperatures

Table 1 Isothermal-crystallization kinetic parameters obtained using Avrami approach

PK/PA-6	T_c (°C)	$t_{1/2}$ (min)	Avrami constants		PK/PA-6	T_c (°C)	$t_{1/2}$ (min)	Avrami constants	
			k (min^{-1})	n				k (min^{-1})	n
100/0	190	0.403	28.18	2.54	50/50	192	0.390	4.37	2.00
	192	0.701	5.89	2.39		194	0.525	3.09	2.30
	194	1.090	3.39	2.35		196	0.805	1.02	1.78
	196	1.987	0.99	1.85		198	1.803	0.18	2.17
	198	2.876	0.49	1.84		200	3.294	0.06	2.01
90/10	192	0.298	7.94	2.23	30/70	192	0.299	14.45	2.37
	194	0.406	4.90	2.38		194	0.459	4.27	2.24
	196	0.676	1.41	2.39		196	0.766	1.55	2.67
	198	1.056	0.60	1.87		198	1.126	0.51	3.05
	200	2.216	0.15	1.93		200	1.802	0.13	2.87
70/30	192	0.370	4.47	1.88	0/100	196	0.394	7.24	2.51
	194	0.519	2.45	2.03		198	0.485	30.2	2.07
	196	0.744	1.20	2.02		200	0.895	0.89	2.38
	198	1.314	0.41	1.92		202	1.664	0.28	2.55
	200	2.617	0.11	1.90		204	2.391	0.07	2.59

The values of n were almost constant between 1.8 and 3.1 for the PK and the PK/PA-6 blends in spite of the different composition and crystallization temperature, suggesting that the crystallization kinetics of PK and PK/PA-6 blends correspond to 3D truncated spherulitic growth with thermal nucleation[32–34]. However, the values of k for the blends were overall increased compared with those of neat PK at the same crystallization temperature. The introduction of PA-6 did not change the crystallization mechanism but the crystallization rate of PK was accelerated with the addition of PA-6.

One of the most important parameters—the crystallization half-time ($t_{1/2}$), which is defined as the time required for the relative degree of crystallinity of the sample to reach 50%—can be obtained directly from the curve. The value of $t_{1/2}$ directly indicates the rate of the crystallization process, and the reciprocal of the crystallization half-time is commonly used to compare the crystallization rates of different systems. The $t_{1/2}$ values of the samples at various crystallization temperatures are summarized in Table 1, and Fig. 10 shows the relationship between T_c and $t_{1/2}$ for different blend compositions. As expected, for all compositions, $t_{1/2}$ increased with increasing the crystallization temperature. The $t_{1/2}$ values of the blends were shorter than the corresponding value for pure PK. These results suggest that overall, the isothermal-crystallization rates of the PK/PA-6 blends at the same crystallization temperature were far higher than those of PK. It is considered that the addition of PA-6 significantly affected the crystallization rate of PK.

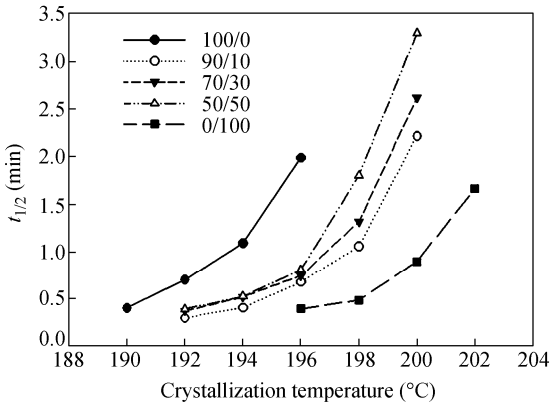


Fig. 10 Crystallization half-time at various T_c for PK/PA-6 blends

Growth Rate of Spherulite and Nucleation

Spherulites constitute the most common morphological texture of polymers crystallized from the melt. The nucleation and crystallization kinetics controls the spherulitic texture, which in turn can greatly affect the mechanical properties of the polymer.

The morphology and spherulitic growth rate are expected to be strongly influenced by the crystallization temperature and the presence of the PA-6 component in the blend. Spherulite growth was observed at different time at 196 °C. Figure 11 indicates the crystal growth of PK at 196 °C with increasing time. The average growth rate of spherulite was calculated, and the results are shown in Fig. 12. The Avrami exponents obtained in the isothermal experiments suggest that the growth in the blends was two- or three- dimensional nucleation, which is likely heterogeneous and instantaneous. When multiple photomicrographs were taken at time intervals, it was observed that the majority of the spherulites were formed instantaneously, and several spherulites appeared at ~10 s. All the spherulites continued to grow at nearly identical growth rates[35, 36]. These minute observations are consistent with heterogeneous blends, which were suggested by the Avrami exponents obtained in the isothermal DSC experiments. In pristine PK, the spherulite growth rate was ~0.32 μm/s. The growth rate was gradually increased by the addition of PA-6, but the spherulites became smaller, as shown in Figs. 12 and 13.

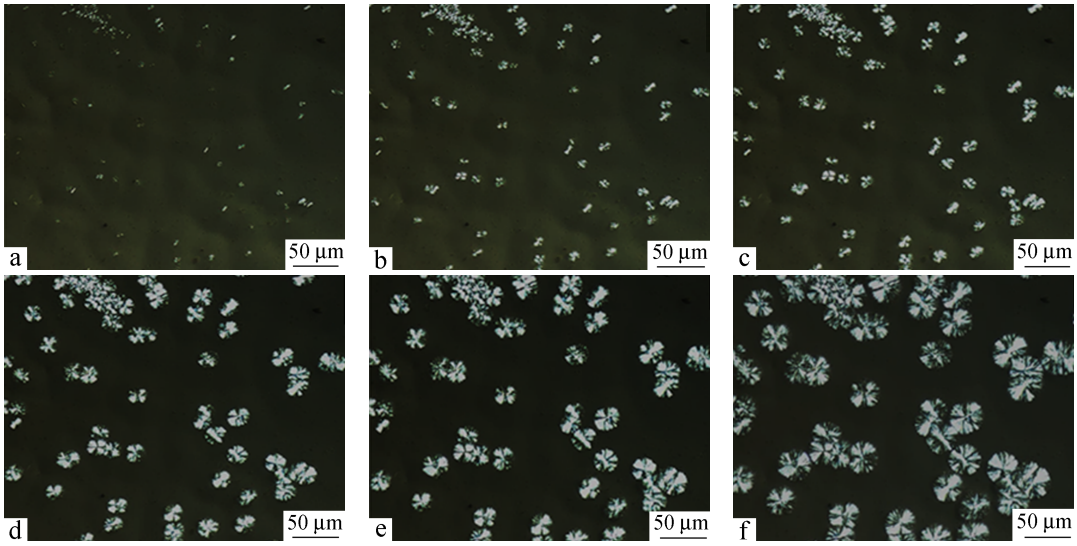


Fig. 11 POM images for PK/PA-6 (90/10) during isothermal crystallization (a: 10 s, b: 20 s, c: 30 s, d: 50 s, e: 60 s and f: 90 s) at 196 °C

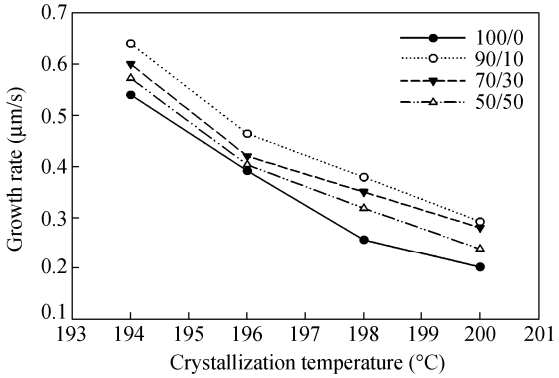


Fig. 12 Spherulitic growth rate of PK/PA-6 blends as a function of the crystallization temperature

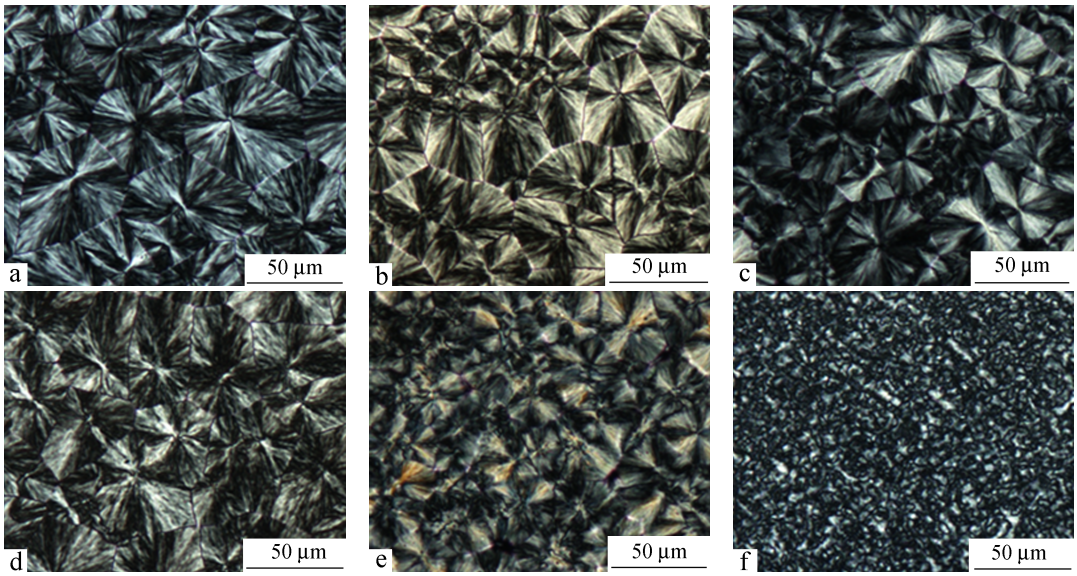


Fig. 13 POM images of PK/PA-6 blends after isothermal crystallization at 196 °C: (a) 100/0, (b) 90/10, (c) 70/30, (d) 50/50, (e) 30/70 and (f) 0/100

As shown in Fig. 13, the spherulite diameter of PK was approximately 30–70 μm. As the PA-6 content increased up to 50 wt%, the size of the spherulites slightly decreased. The size of spherulites decreased and the number of spherulites increased in the blends of PK/PA-6 50/50. In this system, the growth rate and size of the spherulites are expected to be influenced by the isothermal crystallization and the PA-6 content, which are represented precisely by the Avrami constant k and $t_{1/2}$ (Table 1). The k, $t_{1/2}$ and the size of spherulites of the blends gradually decreased as the PA-6 content increased[36–38]. It is considered that the addition of PA-6 did not change the crystallization mechanism of PK but increased the crystal-growth rate.

CONCLUSIONS

The crystallization kinetics and spherulite growth of miscible blends of an aliphatic PK and PA-6 were investigated. A single glass transition was observed, and its composition dependence was described well using the Kwei relation. The crystallization kinetics were strongly influenced by the crystallization temperature and PA-6 content of the blends. The isothermal-crystallization kinetics of PK and the PK/PA-6 blends were described well using the Avrami approach. The melting point of PK was greatly depressed when the PA-6 content of the blend increased. The values of the equilibrium melting temperature of crystalline polymers were used to obtain the Flory-Huggins interaction parameter of the blends. The resulting value was $\chi_{12} = -0.72$, which indicates thermodynamic miscibility. The Avrami exponent n was almost constant despite differences in the blend composition and crystallization temperature. However, the crystallization rate constant decreased as the temperature increased for both the PK and PK/PA-6 blends. The crystallization rate of the PK/PA-6 blends was higher than that of neat PK at the same crystallization temperature. Thus, we conclude that the addition of PA-6 did not change the crystallization mechanism of PK but promoted the crystal-growth rate. In addition, the spherulitic growth rate increased exponentially as the PA-6 content of the blends increased. The growth rate and size of the spherulites were expected to be influenced by the isothermal-crystallization kinetics and the PA-6 content.

REFERENCES

1 Drent, E. and Budzelaar, P.H.M., Chem. Rev., 1996, 96: 663
2 Sommazzi, A. and Garbassi, F., Prog. Polym. Sci., 1997, 22: 1547
3 Garbassi, F., Sommazzi, A., Meda, L., Mestroni, G. and Sciutto, A., Polymer, 1998, 39: 1503
4 Asano, A., Nishioka, M., Kato, A., Takahashi, Y., Sawabe, H., Arao, M., Sato, S., Sato, H., Izumi, T., Olga, D., Ishikawa, D., Hasegawa, T., Okamura, T., Nagata, K., Hikasa, S. and Iwabuki, H., J. Polym. Prepr., 2008, 49: 682
5 Asano, A., Nishioka, M., Takahashi, Y., Kato, A., Hikasa, S., Iwabuki, H., Nagata, K., Sato, H., Hasegawa, T., Sawabe, H., Arao, M., Suda, T., Isoda, A., Mukai, M., Ishikawa, D. and Izumi, T., Macromolecules, 2009, 42: 9506
6 Kato, A., Nishioka, M., Takahashi, Y., Suda, T., Sawabe, H., Isoda, A., Drozdova, O., Hasegawa, T., Izumi, T., Nagata, K., Hikasa, S., Iwabuki, H. and Asano, A., J. Appl. Polym. Sci., 2010, 116: 3056
7 Schmidtke, B., Hofmann, M., Lichtinger, A. and Roessler, E.A., Macromolecules, 2015, 48: 3005
8 Siciliano, A., Severgnini, D., Seves, A., Pedrelli, T. and Vicini, L., J. Appl. Polym. Sci., 1996, 60: 1757
9 Chang, C.S., Woo, E.M. and Lin, J.H., Macromol. Chem. Phys., 2006, 207: 1404
10 Kwei, T.K., Pearce, E.M., Pennacchia, J.R. and Charton, M., Macromolecules, 1987, 20: 1174
11 Kwei, T.K., J. Polym. Sci., Part C: Polym. Lett., 1984, 22: 307
12 Madbouly, S.A., J. Appl. Polym. Sci., 2007, 103: 3307
13 Hao, C., Zhao, Y., Wang, D. and Lai, G., J. Appl. Polym. Sci., 2012, 123: 375
14 Nishi, T. and Wang, T.T., Macromolecules, 1975, 8: 909
15 Xing, P., Dong, L., An, Y., Feng, Z., Avella, M. and Martuscelli, E., Macromolecules, 1997, 30: 2726
16 Panayiotou, C., J. Polym., 2013, 54: 1621
17 Al-Rawajfeh, A.E., Al-Salah, H.A. and Al-Rhael, I., Jordan J. Chem., 2006, 1: 155
18 Ridhore, A. and Jog, J., J. Appl. Polym. Sci., 2013, 129: 65
19 Meaurio, E., Zuza, E. and Sarasua, J.R., Macromolecules, 2005, 38: 1207
20 Penning, J.P. and Manley, R.S.J., Macromolecules, 1996, 29: 77
21 Song, Q.L., Wen H.Y., Christiansen, J.C., Yu, D.H., Chen, C.S. and Jiang, S.C., Chinese J. Polym. Sci., 2016, 34: 1172
22 Zhao, L.F., Chen, J., Tian, X.J. and Zhang, R.L., Chinese J. Polym. Sci., 2015, 33: 499
23 Wang, G.Y. and Qiu, Z.B., Chinese J. Polym. Sci., 2014, 32: 1139
24 Lu, X.F. and Hay, J.N., Polymer, 2001, 42: 9423
25 di Lorenzo, M.L. and Silvestre, C., Prog. Polym. Sci., 1999, 24: 917
26 Mathias, L.J., Davis, R.D. and Jarrett, W.L., Macromolecules, 1999, 32: 7958
27 Avrami, M., J. Chem. Phys., 1939, 7: 1103
28 Avrami, M., J. Chem. Phys., 1940, 8: 212
29 Madbouly, S.A., Abdou, N.Y. and Mansour, A.A., Macromol. Chem. Phys., 2006, 207: 978
30 Pedemonte, E., Turturro, A. and Semino, G., Thermochim Acta, 1988, 137: 115
31 Chen, E.C. and Wu, T.M., J. Polym. Sci., Part B: Polym. Phys., 2008, 46: 158
32 Wunderlich, B., in “Macromolecular physics, Vol. 2”, Academic Press, New York, 1976
33 Wu, F., Huang, C.L., Zeng, J.B., Li, S.L. and Wang, Y.Z., RSC Adv., 2014, 4: 54175
34 Penning, J.P. and Manley, R.S.J., Macromolecules, 1996, 29: 84
35 Wang, B., Wang, W., Wang, H. and Hu, G., J. Polym. Res., 2010, 17: 429
36 Zhang, F., Zhou, L., Xiong, Y., Liu, G. and Xu, W., J. Appl. Polym. Sci., 2009, 111: 2930
37 Ellis, T.S., Macromolecules, 1989, 22: 742
38 Weng, W., Chen, G. and Wu, D., Polymer, 2003, 44: 8119